Article

Processing of Waste Copper Converter Slag Using Organic Acids for Extraction of Copper, Nickel, and Cobalt

Pratima Meshram [1], Uday Prakash [1] , Lalit Bhagat [1], Abhilash [1],* , Hongbo Zhao [2] and Eric D. van Hullebusch [3]

[1] CSIR-National Metallurgical Laboratory, Jamshedpur 831007, India; pmeshram@gmail.com (P.M.); udayprakash8.16@gmail.com (U.P.); lalitbhagat33@gmail.com (L.B.)

[2] School of Minerals Processing & Bioengineering, Central South University, No. 932 Lushan South Road, Yuelu District, Changsha 410083, China; alexandercsu@126.com

[3] Institut de physique du globe de Paris, Université de Paris, CNRS, F-75005 Paris, France; vanhullebusch@ipgp.fr

* Correspondence: abhibios@gmail.com; Tel.: +91-657-2345274

Abstract: An innovative, economical, and environmentally sound hydrometallurgical process has been proposed for recovering Cu, Ni, and Co from copper-rich converter slag by organic acids. In the leaching experiments, the effects of organic acid concentrations, pulp density, temperature, and time were investigated. Optimum recovery of 99.1% Cu, 89.2% Ni, 94% Co, and 99.2% Fe was achieved in 9–10 h at 308 K (35 °C) temperature and 15% pulp density with 2 N citric acid using <45 μm particles. Pourbaix diagrams of metal-water-citrate systems were supplemented to examine solubility of ligands at the desired conditions. Furthermore, the leaching mechanism was based on the SEM-EDS (energy-dispersive X-ray spectroscopy) and XRD characterization as well as the leaching results obtained.

Keywords: converter slag; citric acid; leaching; metal-water-citrate system; selectivity

1. Introduction

A heavy amount of slag (2.2 tons per ton of copper) is generated during the pyro or hydrometallurgical copper production which generally contains significant amounts of some valuable metals such as copper, nickel, cobalt, and iron [1,2]. In the last few decades, there has been growing interest in hydrometallurgical processes to recover valuable metals from smelter slags [3]. In these studies, efforts were mainly focused on the leaching processes with or without some pre-treatments. Various methods using lixiviants such as acids, bases, salts, or their combinations have been developed for base metal extraction from converter slags [4] like H_2SO_4 only, H_2SO_4 with H_2O_2, H_2SO_4 with $NaClO_3$ as oxidant, H_2SO_4 with air as oxidant [5], H_2SO_4 followed by water leaching, roasting with $Fe_2(SO_4)_3$ followed by leaching with H_2O [3,6], oxidative leaching with $K_2Cr_2O_7$ and H_2SO_4 [7,8], bioleaching with lithoautotrophic microorganisms such as *Acidithiobacillus ferrooxidans* [9,10] as well as heterotrophic microorganisms such as *Aspergillus niger* [11] and *Pseudomonas fluorescens* [12].

Banza et al. performed base metal recovery by oxidizing leaching with ground slag samples obtained from Lubumbashi, Democratic Republic of Congo [5]. Metals recoveries of around 60% Cu, 90% Co, 90% Zn, and 90% Fe were obtained after 2 h using only H_2SO_4. When a combination of H_2SO_4 and H_2O_2 was used, metal extractions of more than 80% Cu, 90% Co, 90% Zn, and 5% Fe were recorded. Yang et al. investigated the leaching of copper smelter slag from Guangdong Province of China using the same acid with $NaClO_3$ oxidant and neutralization with $Ca(OH)_2$ for better and faster

filtration of the precipitate [13]. The overall leach and selective precipitation process recovered about 98% Co, 97% Zn, and 89% Cu from this slag, while only 3.2% Si and 0.02% Fe dissolved. Deng and Ling studied the recovery of copper and cobalt from converter slag obtained from Zhongtiaoshan Nonferrous Complex [7]. The dry slag that was used in this investigation was first treated with H_2O_2 and H_2SO_4 (120% stoichiometric quantity) and then aged. The cured slag was then water leached resulting in more than 95% Co and up to 90% Cu recovery. Altundogan and Tumen revealed that the roasting with $Fe_2(SO_4)_3$ of copper converter slag from Etibank Ergani copper works in Maden, Turkey [6] followed by leaching with water brought total recoveries of 93%, 38%, 13%, and 59% for Cu, Co, Ni, and Zn, respectively. Altundogan et al. investigated the extraction characteristics of Cu, Co, Zn, and Fe from copper converter slag obtained from Ergani Copper Plant in Maden, Turkey [4] by oxidative leaching with $K_2Cr_2O_7$ and H_2SO_4 lixiviant. The experimental results indicated that the presence of dichromate has a large influence on the extraction of metals. The process recovered 81.15% Cu, 12.0% Co, 3.15% Fe, and 10.27% Zn. Mehta et al. investigated the recovery of Co, Ni, and Cu from two copper converter slag samples of Indian Copper Complex (ICC) Ghatsila, India by bio-leaching using *Acidithiobacillus ferrooxidans* [9]. Recoveries for sample 1 were found to be 98% Cu (50 days), 60% Ni (75 days), and 80% Co (75 days), while sample 2 resulted in 99% Cu (80 days), 22% Ni (70 days), and 30% Co (50 days). In leaching with *Aspergillus niger,* maximum recoveries of Cu, Co, Ni, and Fe were 78.50%, 90.0%, 45.50%, and 40.15%, respectively, as recorded by Sukla et al. [11]. All these methods suffer from sulfur dioxide emission, low metal recovery, poor economics, and the additional cost of furnaces and roasters as well.

The present study aimed to develop an environmentally sound and economically competitive approach for recovering metal values from such a slag, where organic acids (oxalic acid and citric acid) have been preferred over inorganic acids. Leaching of lead and copper by citric acid from direct-to-blister copper flash smelting slag was carried out by Gargul et al. [14], wherein the slag had a high degree of difference in chemistry due to differences in temperature used for processing and enriched content of Pb and Cu. The convertor slag used in our study pertains to extraction of a reduced concentration of Cu present and traces of Pb (left unattended). In regard to that, the effect of acid concentration, pulp density, temperature, and time were investigated. The solubility of the metal-water-citrate system was established. The recoveries of metals were corroborated with the SEM and XRD of head and leach residue samples to evaluate the association of copper in the matrix and the underlying mechanism for selective dissolution of copper.

2. Materials and Methods

2.1. Materials

Copper converter slag supplied by Birla Copper, Dahej, India was ground. Coning and quartering techniques were performed for homogenization of slag sample. Chemical composition shows the presence of 1.43 wt% Cu, 0.02 wt% Ni, 0.05 wt% Co, 49.92 wt% Fe, and 11.82 wt% SiO_2 in ground converter slag. The sieve analysis of the converter slag and the content of Cu, Ni, Co, and Fe in individual fractions are given in Table 1. Owing to the higher value of 1.38% Cu with particle size <45 μm, this sieve size was preferred for further experiments. By examining the slag samples with optical microscopy (Leica™, Wetzlar, Germany) and by X-ray diffraction (Bruker™, Baden-Württemberg, Germany) analysis, it was found that fayalite, magnetite, and kyanite are the major phases whereas copper silicate, wüstite, oxides of copper, nickel, and cobalt are the available minor phases. Whole area or overall sample analysis was carried out at 15 kV and 160× magnification by Electron Probe Micro Analysis (EPMA) to identify the mass elemental percentage of the contents to obtain an overall idea on the sample composition. The results are depicted in Figure 1a and further analyzed by X-ray energy dispersive spectra (EDAX) in Figure 1b. As regards morphology, the presence of >80% glassy/non-crystalline silicate phase was found, with independent mineral phases of copper, nickel, and cobalt. Nickel was seen associated with magnetite and metallic copper. Iron in the slag was

present as magnetite, fayalite, and kyanite. Silicate in the slag was also contributed by both fayalite and kyanite. The overall image presented in Figure 1 was then targeted at respective desired points designated by visual differences as in Figure 2 and identified in Table 2.
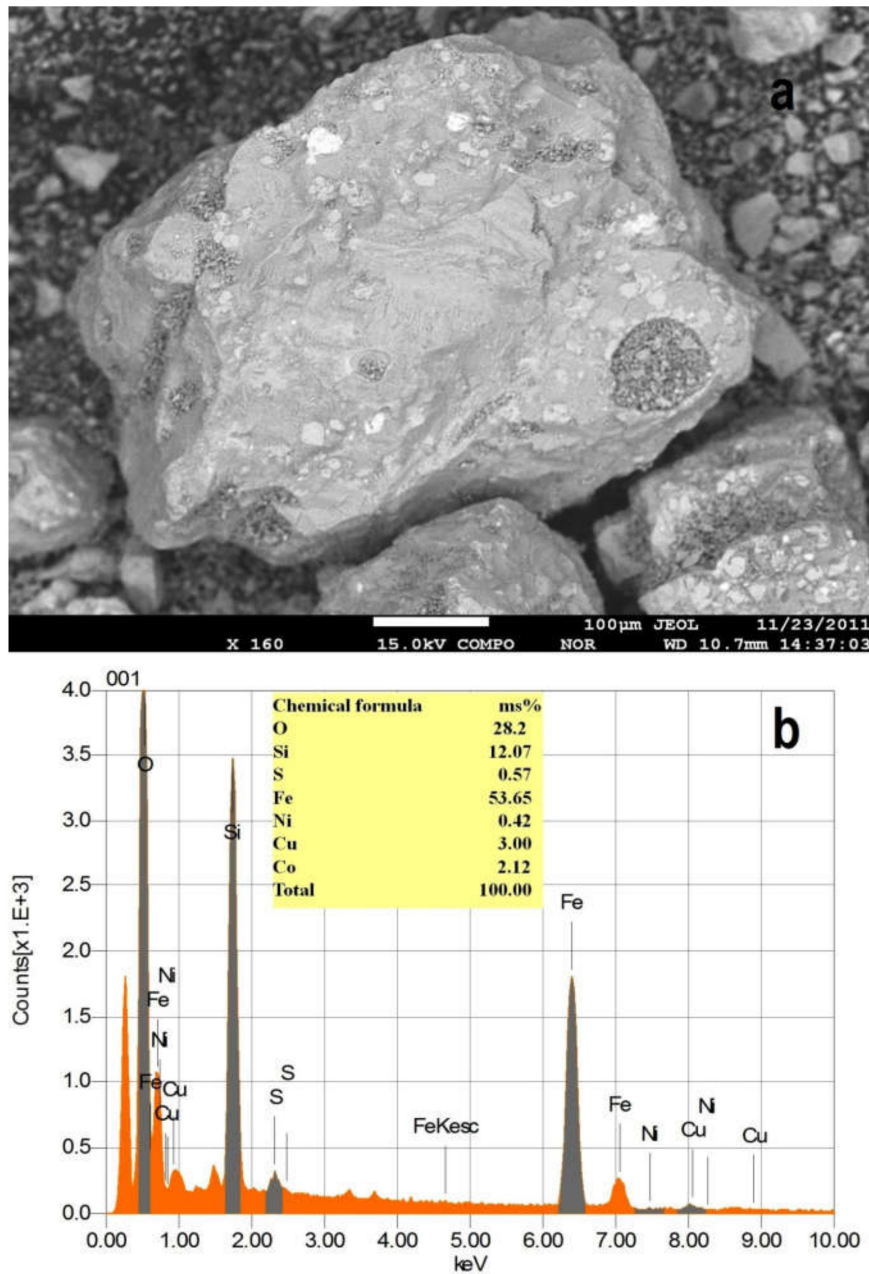

Figure 1. Electron Probe MicroAnalysis (EPMA)-EDAX (energy-dispersive X-ray spectroscopy) (JX-8530, JEOL™, Tokyo, Japan) of converter slag overall sample, (**a**) micrograph; (**b**) EDS spectra (ms%: mass percentage).

Table 1. Sieve analysis of different fractions of converter slag.

Sieve Size (µm)	Cu	Ni	Co	Fe	SiO₂
	wt%	wt%	wt%	wt%	wt%
<150	0.96	0.009	0.01	36.49	6.98
150–105	0.99	0.01	0.02	38.41	8.33
105–75	1.08	0.01	0.03	43.16	9.88
75–45	1.19	0.015	0.04	46.33	10.47
<45	1.38	0.02	0.05	49.92	11.82
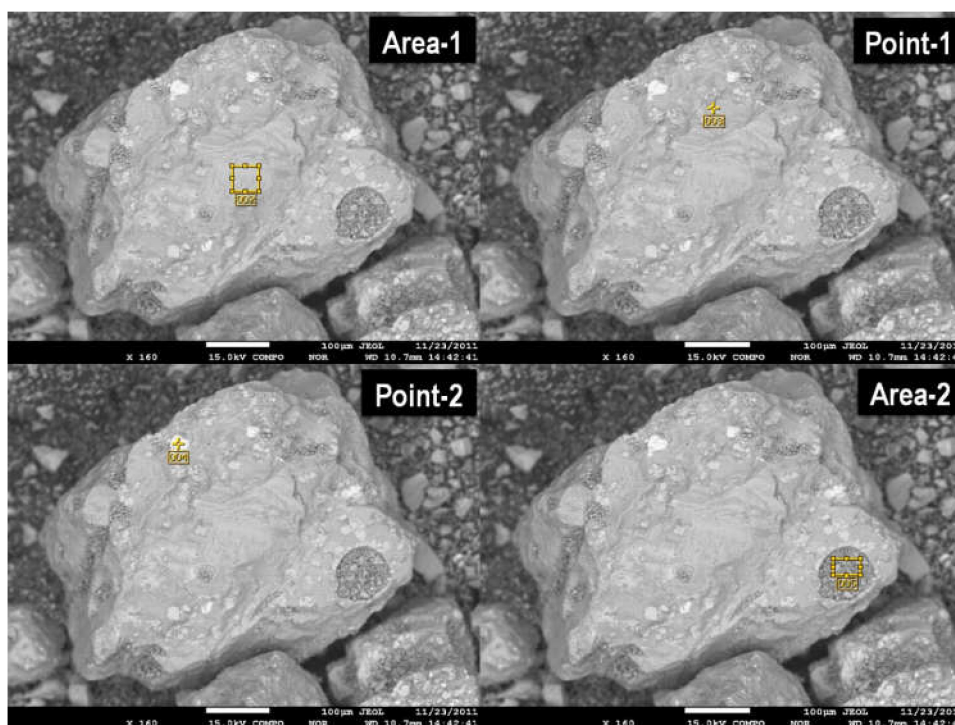
Figure 2. Respective marked areas/points of image in Figure 1 analyzed under EPMA.

Table 2. EPMA-EDS analysis of areas/points marked in Figure 2 (ms%—mass percentage).

Chemical Formula	Area 1	Point 1	Point 2	Area 2
	ms%	ms%	ms%	ms%
O	29.01	34.68	35.43	26.64
Fe	55.16	50.71	47.17	58.41
Si	14.11	13.28	14.96	13.16
Cu	0.6	0.27	0.35	0.22
Ni	0.11	0.14	0.17	0.09
S	0.1	0.12	0.91	0.59
Co	1.11	1..08	1.10	1.09
Total	100	100	100	100

Additional sections were focused on in order to get a better idea of the mineral association, as depicted in Figure 3. The lustrous mineral grain in Figure 3a was less oxidic and could be designated as a pure copper mineral as evident from its composition; whereas the rise in non-oxidic minerals in Figure 3b significantly decreased copper content and increased iron content.
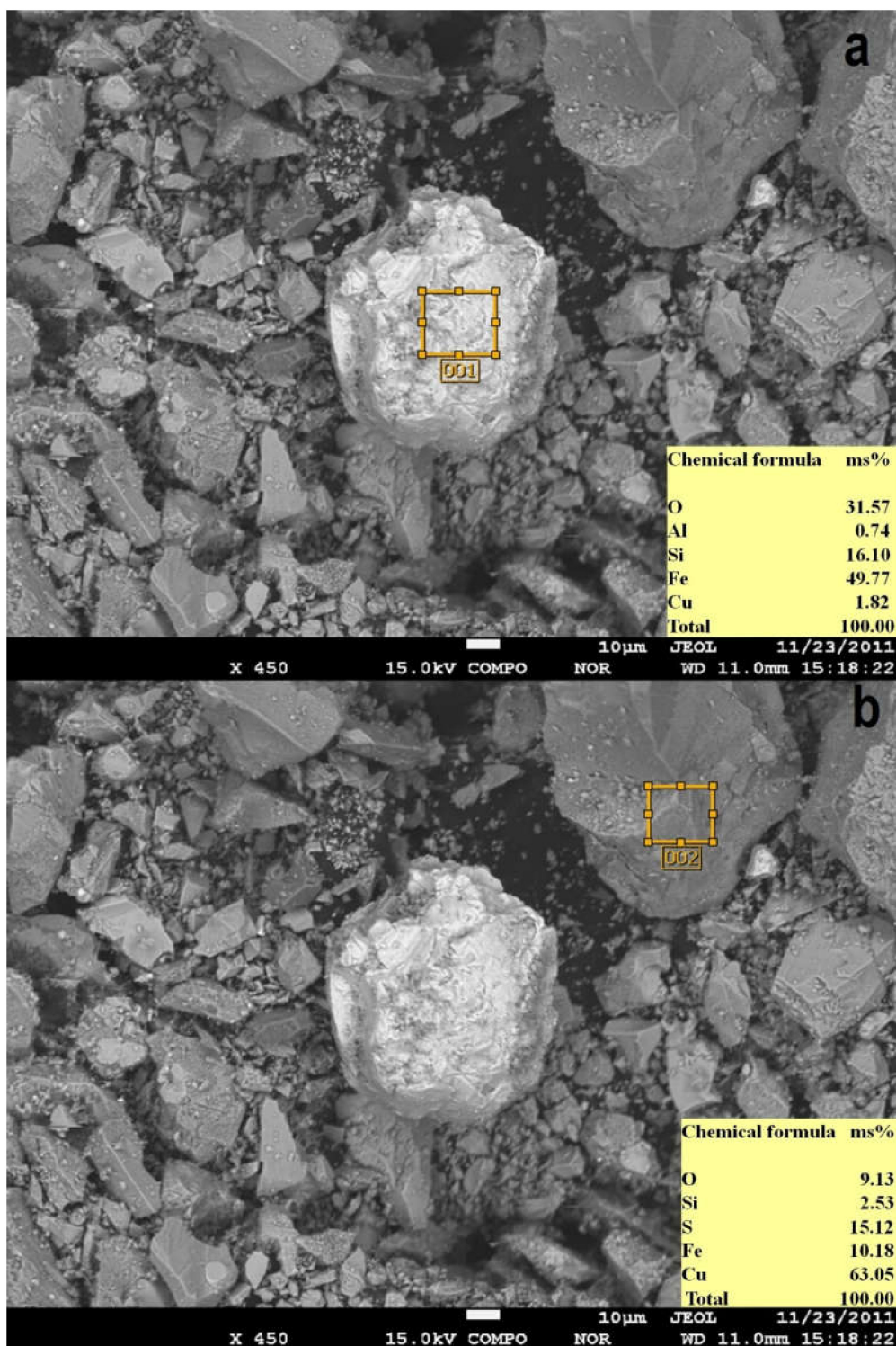
Figure 3. Association of copper in converter slag vis-à-vis the presence in (**a**) oxidic and (**b**) non-oxidic phases (ms%—mass percentage).

2.2. Methods

Leaching was carried out in 250–500 mL conical flasks containing 100 mL of an organic acid with varied concentrations (0.5–3.0 N) and 5–20 g of <45 μm copper converter slag. Experimental flasks were incubated on a rotary shaker at 120 rpm for 0.5–15 h at 308–328 K (35–55 °C). On termination of the experiment, the values of pH and E_h were measured with a pH-millivolt meter and contents

of the flasks were filtered [15] using Whatman No. 42 paper. All the chemicals were of analytical grade from Merck (Germany) and all aqueous solutions were prepared with deionized water. The pH of the aqueous solutions was adjusted by adding NaOH or H_2SO_4. Ferrous ion was determined by volumetric analysis with potassium dichromate. Upon termination of the leaching experiments, the slurry was filtered, solid residues were dried, and samples were taken for chemical analysis as well as mass balance. The concentration of metals in the leach liquor was determined using an atomic absorption spectrometer (GBC-980™, GBC, VIC, Australia) and inductively coupled plasma optical emission spectroscopy ICP-OES (VISTA-MPX™, Varian, Palo Alto, CA, USA) after required dilution. The leaching results presented in the paper are from the average of duplicate experiments (with max. ±2% deviation) conducted under the same conditions.

3. Results

3.1. Oxalic Acid Leaching of Copper Converter Slag

Leaching tests were carried out at 308 K (35 °C) temperature using 5% pulp density. The concentration of oxalic acid varied from 0.5 to 2 N. Figure 4 shows a characteristic curve for the reacted fraction of Cu, Ni, Co, and Fe during 15 h leaching duration at 120 rpm. The maximum recovery of Cu, Co, and Fe were found to be 2.4%, 15.2%, and 11.4%, respectively, by using 2 N oxalic acid, while 27.5% Ni were obtained using 0.5 N oxalic acid (Figure 4). The presence of oxalate ions reduced the stability region of the copper oxides [16].
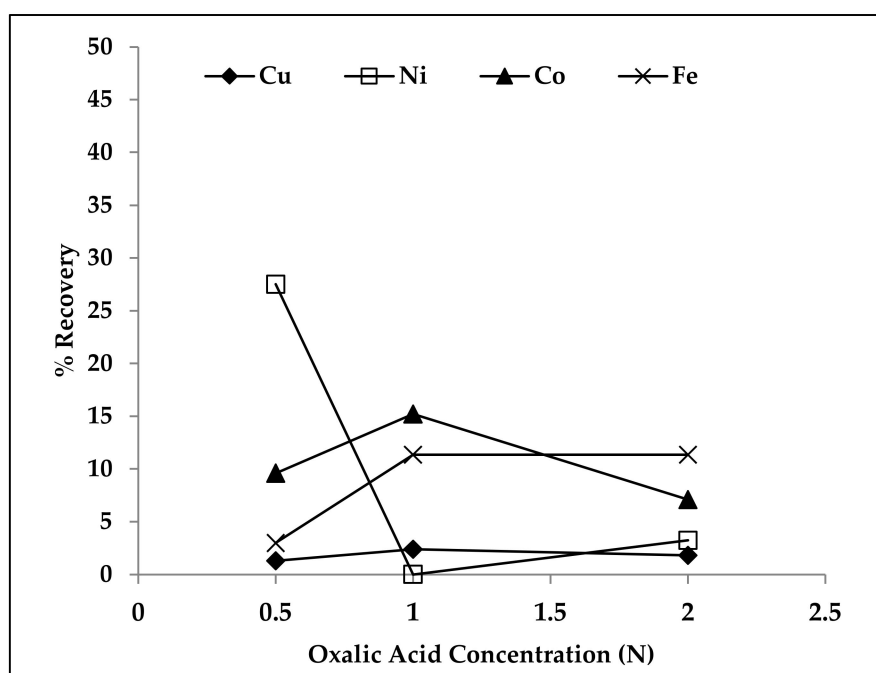

Figure 4. Effect of acid concentration of oxalic acid on Cu, Ni, Co and Fe recovery at 5% pulp density (PD), 308 K in 15 h.

3.2. Citric Acid Leaching of Copper Converter Slag

The effect of acid concentration on the recovery of metals from copper converter slag was studied at 5% pulp density (*w/v*), 308 K temperature, and 120 rpm. Figure 5 shows an increase in Cu, Ni, Co, and Fe recovery with an increase in acid concentration up to 2 N after which it decreased. It was further observed that the maximum recovery of Cu, Ni, Co, and Fe was found to be 99.0%, 89.2%, 94%, and 99.2% with 2 N citric acid. All the experiments were performed for 15 h. Citric acid is believed to attack preferentially better on minerals involving a hydrogen ion attack and chelation of the dissolved metallic ions [16]. Hence, citric acid with an optimal concentration of 2 N was opted for further studies.
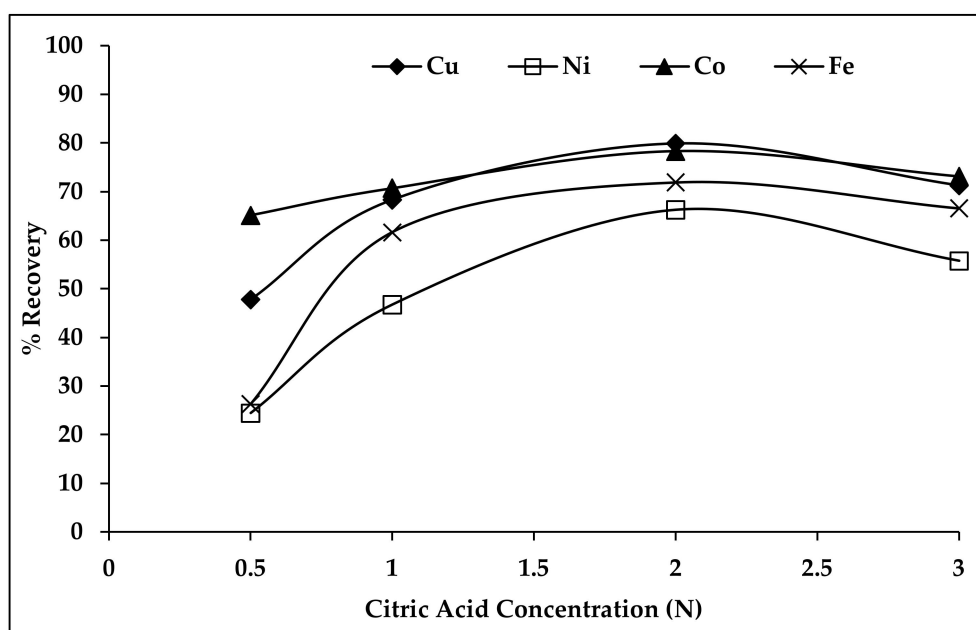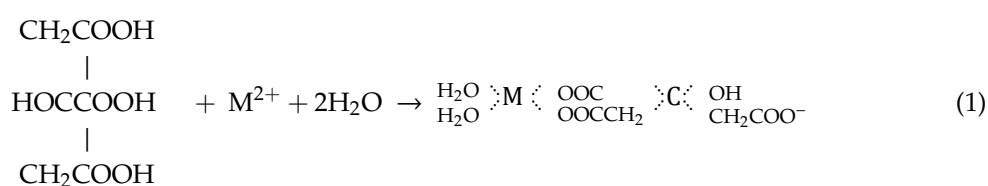
Figure 5. Effect of acid concentration of citric acid on Cu, Ni, Co, and Fe recovery at 5% PD, 308 K in 15 h.

The metals (M) reacted with citric acid to form soluble metal chelates, and the reaction was expressed as Equation (1):

$$\begin{array}{c} CH_2COOH \\ | \\ HOCCOOH \\ | \\ CH_2COOH \end{array} \quad + M^{2+} + 2H_2O \rightarrow \begin{array}{c} H_2O \\ H_2O \end{array} M \begin{array}{c} OOC \\ OOCCH_2 \end{array} C \begin{array}{c} OH \\ CH_2COO^- \end{array} \qquad (1)$$

The chelation of metal ions by organic acid through a combined method of acidolysis and complexolysis improves the recovery of Co, Ni, and Fe; whereas it did not find itself specific for copper. The concentration of copper after leaching was relatively higher, clearly stating lower metal amenability (no chelation) by citric acid. The citrate-ion changes the copper speciation which takes place due to the electrostatic attraction between them. The aqueous citrate (L = ligand, $C_6H_5O_7^{3-}$) ions exist in four major phases as L^{3-}, HL^{2-}, H_2L^-, and H_3L. Similarly, the aqueous copper ions and their citrate ions form complexes as Cu^{2+}, CuL^-, $CuHL^0$, CuH_2L^+, and $Cu(OH)L^{2-}$. The predominance curve was studied, and it was observed that the citrate ion is highly protonated [16] below pH 2.0. In addition, the CuL^{1-}-complex is the dominated phase in the pH range of 3–4, while $Cu(OH)L^{2-}$-complex phase is generated above pH 4. Due to the high stability of the Cu-ligand, its complex remains in the solution at a higher pH.

3.3. Pourbaix Diagram of Copper-Citrate System

The Pourbaix diagram for the copper citrate system was established to examine the occurrence of Cu-citrate complex at different pH and redox potential (Eh), thermodynamically. To draw the diagram, different useful relations were used, like the Nernst equation using Gibbs free energy and stability constants for formation of aqueous citrate (L = ligand) species L^{3-}, HL^{2-}, H_2L^-, H_3L; the aqueous copper species Cu^{2+}, CuL^-, $CuHL^0$, CuH_2L^+, $Cu(OH)L^{2-}$; and the solid copper species Cu, CuO, Cu_2O, $Cu(OH)_2$ on the basis of reactions and its rate constant from Table 2. Figure 6a shows the Pourbaix diagram of the Cu-water system, whereas, the presence of Cu-citrate ligands changed the solubility diagram as shown in Figure 6b.
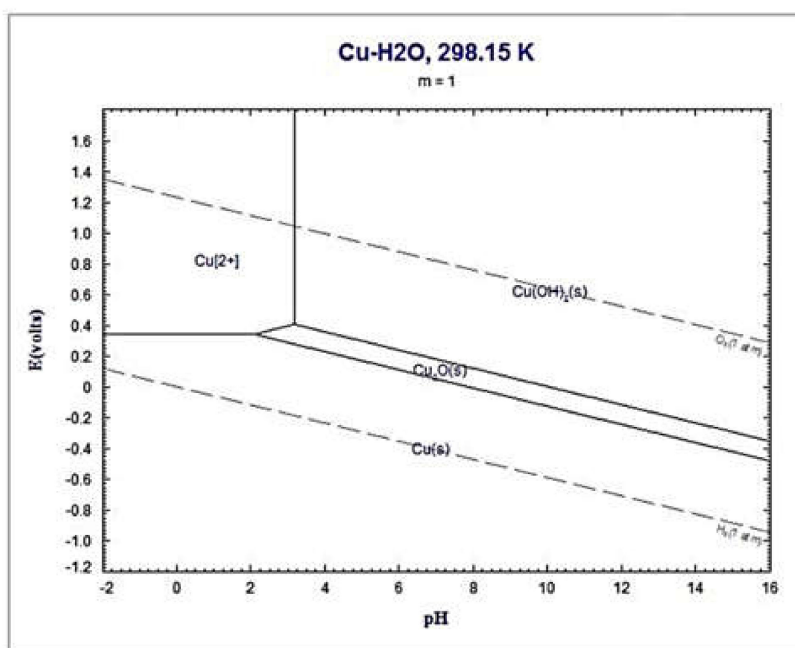
(a)
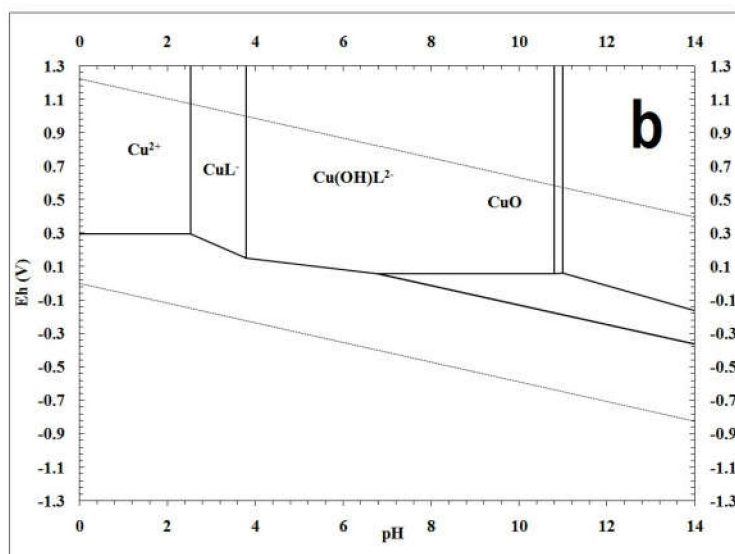
(b)

Figure 6. Pourbaix diagram for (a) Cu-H$_2$O system; (b) Cu-H$_2$O-citrate system at 298 K (total copper activity = 1 M, total citrate activity = 0.667 M).

While performing the experiments, we noted Eh-pH values corresponding to time which shows the rise in redox potential from 40 mV to 321 mV (pH 1.98 to 2.77) indicating a higher oxidizing environment for metal dissolution. Due to the presence of an acidic medium in the solution, the copper metal oxidizes to form metal ions as in Equation (2) and concurrently represented in Figure 6a.

$$Cu \rightarrow Cu^{2+} + 2e^- \tag{2}$$

The reaction of copper ions with citrate ligand present in solution is represented in Equations (3)–(5) and the chemical species governing are shown in Table 3:

$$Cu^{2+} + C_6H_8O_7 \rightarrow CuC_6H_5O_7{}^+ + H^+ \tag{3}$$

$$Cu^{2+} + C_6H_7O_7{}^- \rightarrow CuC_6H_6O_7 + H^+ \tag{4}$$

$$Cu^{2+} + C_6H_6O_7{}^{2-} \rightarrow CuC_6H_5O_7{}^- + H^+ \tag{5}$$
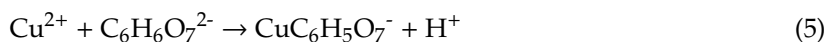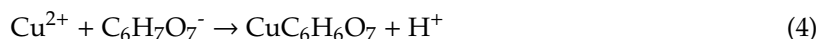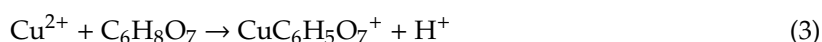
Table 3. Equilibrium constants for citric acid and copper citrate complexes at 298 K.

Reaction	Log K
$H^+ + L^{3-} \leftrightarrow HL^{2-}$	6.29
$2H^+ + L^{3-} \leftrightarrow H_2L^{1-}$	11.23
$3H^+ + L^{3-} \leftrightarrow H_3L$	14.41
$Cu^{2+} + L^{3-} \leftrightarrow CuL^{1-}$	5.95
$Cu^{2+} + H^+ + L^{3-} \leftrightarrow CuHL^0$	8.68
$Cu^{2+} + 2H^+ + L^{3-} \leftrightarrow CuH_2L^+$	11.34
$Cu^{2+} + H_2O + L^{3-} \leftrightarrow Cu(OH)L^{2-} + H^+$	2.16

From Eh-pH diagram in Figure 6b, Eh and pH correspond to 0.321 V and 2.77 V, respectively, and lie in the CuL⁻ region after 15 h of leaching, concluding the formation and stability of copper citrate complex as shown in Equation (5). Thus, $CuC_6H_5O_7{}^{1-}$ compound exists in final leach liquor as a stable complex resulting in more than 99% extraction of copper ions from slag.
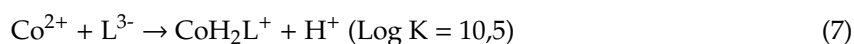
3.4. Pourbaix Diagram of Cobalt-Citrate System

The Pourbaix diagram for the cobalt-citrate system was established to examine the occurrence of Co-citrate complex at different pH and redox potential (Eh), thermodynamically. To draw the diagram, different useful relations were used like the Nernst equation using the Gibbs free energy and stability constants for formation of aqueous citrate (L = ligand) species. Figure 7a shows the Pourbaix diagram of the Co-water system, whereas, the presence of Co-citrate ligands changed the solubility diagram as shown in Figure 7b.

Due to the presence of an acidic medium in the solution, the cobalt metal oxidizes to form metal ions as shown in Equation (6) and concurrently represented in Figure 7a.
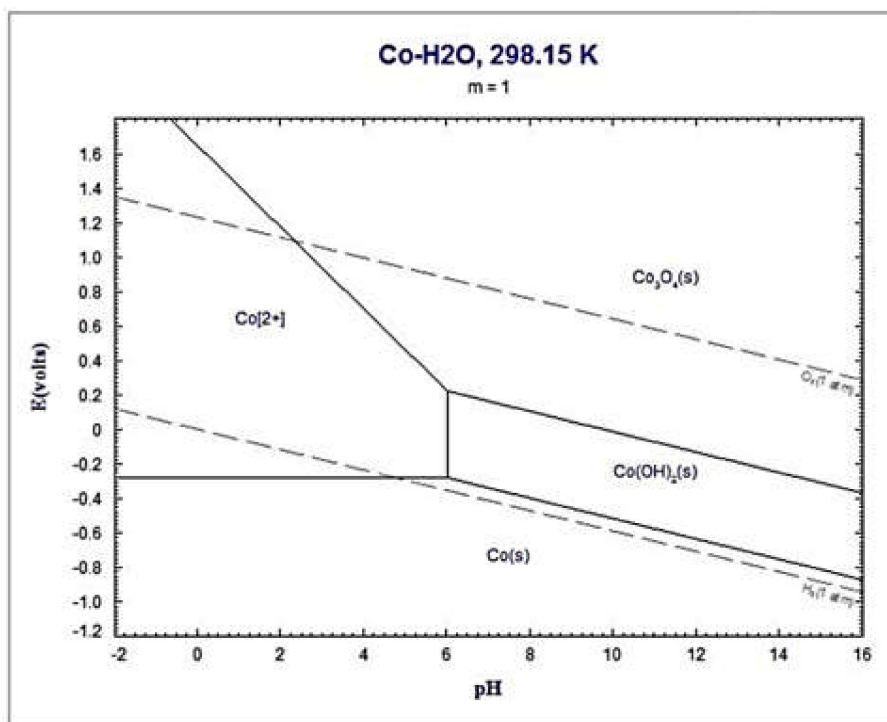
$$Co \rightarrow Co^{2+} + 2e^- \tag{6}$$

The reaction of cobalt ions with citrate ligand present in the solution is represented in Equation (7):

$$Co^{2+} + L^{3-} \rightarrow CoH_2L^+ + H^+ \text{ (Log K = 10,5)} \tag{7}$$

From Eh-pH diagram in Figure 7b, 2.77 pH and 0.337 V Eh correspond to CoH_2L^+ which is a stable soluble compound.

3.5. Pourbaix Diagram of Nickel-Citrate System

The Pourbaix diagram for the nickel-citrate system was established to examine the occurrence of Ni-citrate complex at different pH and redox potential (Eh), thermodynamically. To draw the diagram, different useful relations were used like the Nernst equation using the Gibbs free energy and stability constants for formation of aqueous citrate (L = ligand) species. Figure 8a shows the Pourbaix diagram of the Ni-water system, whereas, the presence of Ni-citrate ligands changed the solubility diagram as shown in Figure 8b.
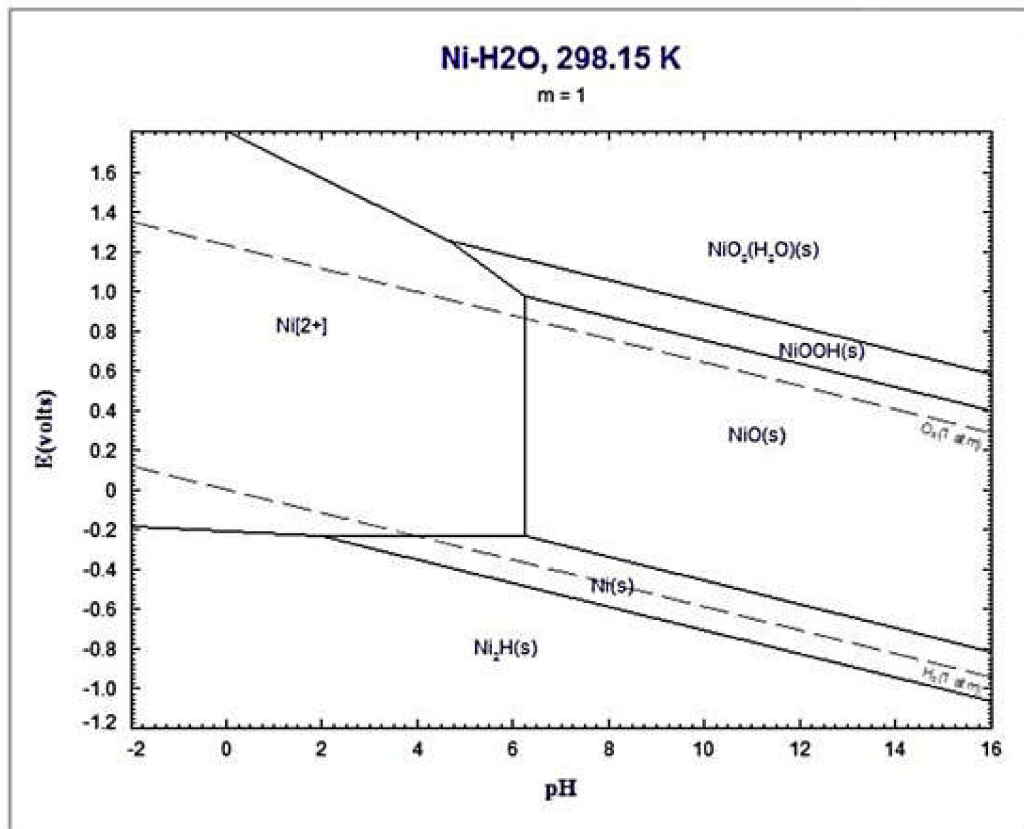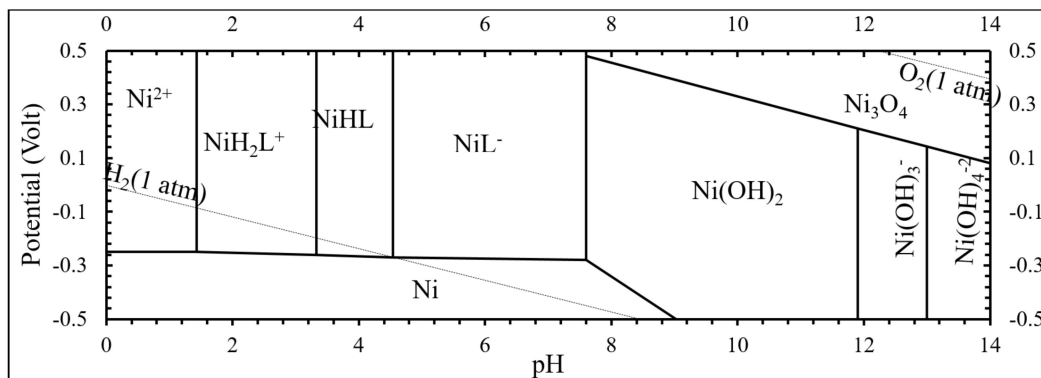
(**a**)
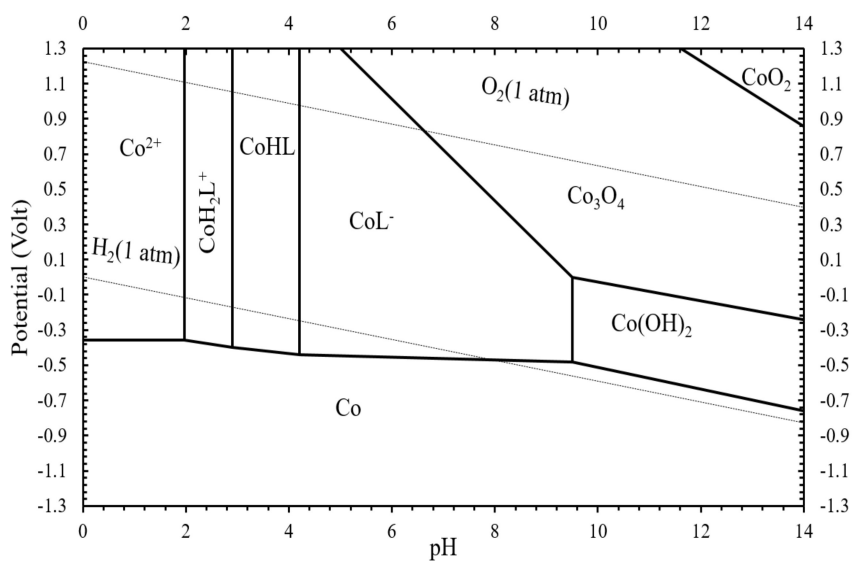
(**b**)

Figure 7. Pourbaix diagram for (**a**) Co-H$_2$O system; (**b**) Co-H$_2$O-citrate system at 298 K (total cobalt activity = 1 M, total citrate activity = 0.667 M).
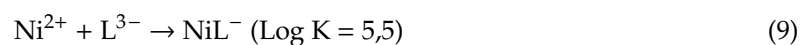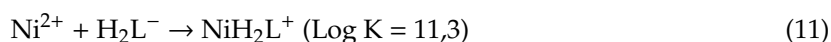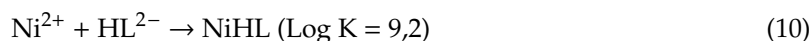
(a)

(b)

Figure 8. Pourbaix diagram for (**a**) Ni-H$_2$O system; (**b**) Ni-H$_2$O-citrate system at 298 K (total nickel activity = 1 M, total citrate activity = 0.667 M).

Due to the presence of an acidic medium in the solution, the nickel metal oxidizes to form metal ions as shown in Equation (8) and concurrently represented in Figure 8a.

$$Ni \rightarrow Ni^{2+} + 2e^- \tag{8}$$

The reaction of nickel ions with citrate ligand present in solution is represented in Equations (9)–(11):

$$Ni^{2+} + L^{3-} \rightarrow NiL^- \ (Log \ K = 5,5) \tag{9}$$

$$Ni^{2+} + HL^{2-} \rightarrow NiHL \text{ (Log K = 9,2)} \tag{10}$$

$$Ni^{2+} + H_2L^- \rightarrow NiH_2L^+ \text{ (Log K = 11,3)} \tag{11}$$

From Eh-pH diagram in Figure 8b, 2.77 pH and 0.337 V Eh correspond to NiH_2L^+ which is a stable soluble compound.

3.6. Pourbaix Diagram of Iron-Citrate System

The Pourbaix diagram for the nickel-citrate system was established to examine the occurrence of Fe-citrate complex at different pH and redox potential (Eh), thermodynamically. Due to the presence of an acidic medium in the solution, the nickel metal oxidizes to form metal ions as shown in Equation (12).

$$Fe \rightarrow Fe^{2+} + 2e^- \tag{12}$$

The reaction of nickel ions with citrate ligand present in the solution is represented in Equation (13):

$$Fe^{2+} + L^{3-} \rightarrow FeH_2L^+ + H^+ \text{ (Log K = 10.8)} \tag{13}$$
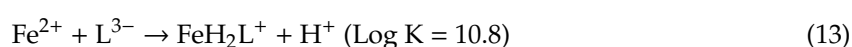
It can be concluded that 2.77 pH and 0.337 V Eh correspond to FeH_2L^+ which is a stable soluble compound; this can be corroborated with previous studies [17].

3.7. Effect of Pulp Density

To determine the effect of solid content in the suspension (pulp density) on the efficiency and rate of chemical leaching of metals from converter slag, experiments at different pulp densities were performed. The experiments were carried out at the previously accepted acid concentration (i.e., 2 N), for 15 h at 120 rpm and 308 K (35 °C) temperature. The solid copper converter slag was introduced to obtain pulp density of 5%, 10%, 15%, and 20% for leaching. The results are represented in Figure 9 which shows that the conversion of metals increases as the pulp density increases. A maximum of 99.1% Cu, 89.2% Ni, 94% Co, and 99.2% Fe was recovered by 15% pulp density. When raising the pulp ratio to 20%, the recoveries fell, which could be attributed to the rise in pH of solution inhibiting metal recovery owing to the lesser availability of reactive citrate ions [10] (Table 4).
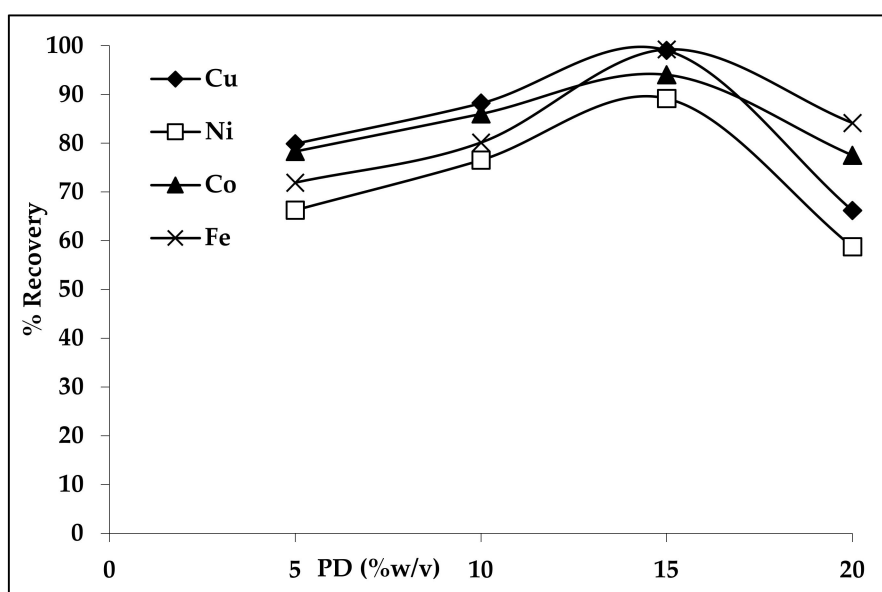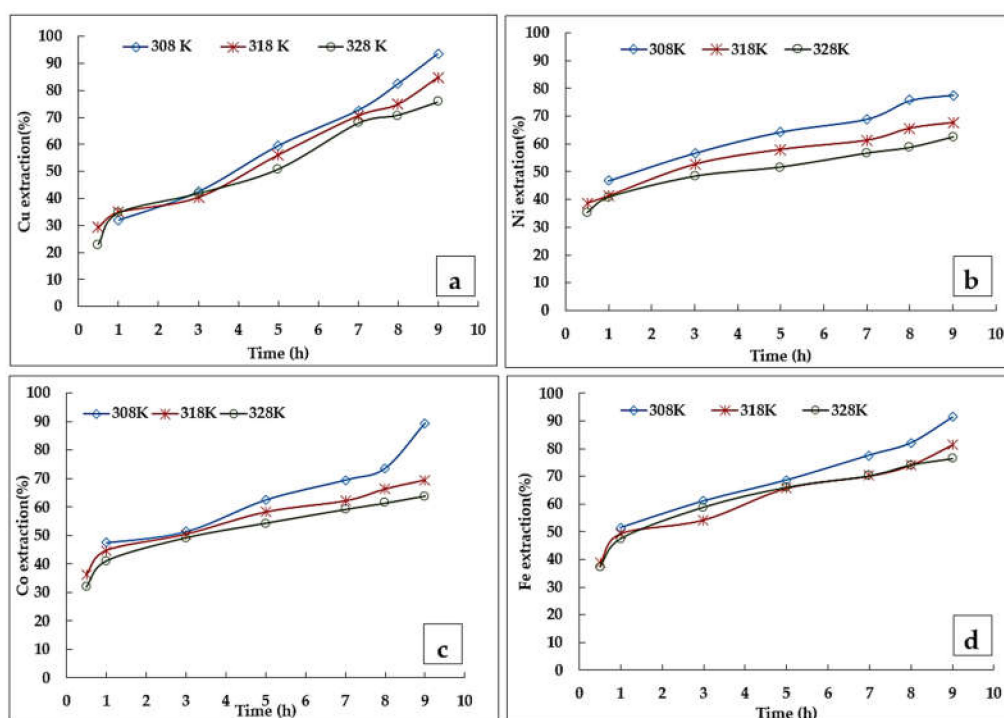

Figure 9. Effect of pulp density on recovery of Cu, Ni, Co, and Fe at 308 K using 2 N citric acid for 15 h.

Table 4. Initial and final pH of slurry with 2 N citric acid in varying pulp densities of slag at 308 K.

Conditions	Final pH					
	1 h	**3 h**	**6 h**	**9 h**	**12 h**	**15 h**
5% PD	1.98	2.08	2.13	2.26	2.38	2.49
10% PD	2.12	2.23	2.42	2.55	2.76	2.82
15% PD	2.21	2.39	2.44	2.69	2.81	2.98
20% PD	2.33	2.76	3.03	3.75	4.19	4.26

3.8. Effect of Time

Experiments were performed with 15% pulp density at 120 rpm with 2 N citric acid at 308 K (35 °C) temperature which is shown in Figure 10. The optimum recovery of these metals was 99.0%, 89.2%, 94%, and 99.2%, respectively, at 308 K (35 °C), 15% pulp density, 2 N citric acid in 15 h where a maximum redox potential of 321 mV was recorded; the recovery of Cu, Ni, Co, and Fe was almost marginally changed after 9 h onwards. It can be concurrently stated that the optimum time for leaching was 9 h, after which a steady-state was achieved. The progressive recovery of Cu, Ni, Co, and Fe with leaching time was studied and Eh-pH values were noted. It was observed that the redox potential rose up to 300 mV in 9 h with pH gradually decreasing from 3.5 to 1.98 which can be seen from the recoveries of 97.5%, 86.7%, 91.6%, and 97.6%, respectively, for Cu, Ni, Co, and Fe in 9 h.

Figure 10. Effect of time on recovery of (**a**) Cu, (**b**) Ni, (**c**) Co, and (**d**) Fe at 15% pulp density with 2 N citric acid at various temperatures.

3.9. Effect of Temperature

Temperature is known to be the most important parameter affecting the rates of reactions. Effect of temperature on the dynamics of leaching of metals from copper converter slag was therefore investigated. The experiments were carried out at the parameter values determined previously: 2 N citric acid, 15% pulp density (*w/v*), 9 h. The experimental results of metals recovery during leaching of converter slag are presented in Figure 11. It depicts that the rate and efficiency of metal recovery decreased with an increase in temperature. The rise in temperature from 308 K (35 °C) to 328 K (55 °C)

resulted in a decrease in the conversion of more than 0.5-fold Cu and 0.35-fold Ni, and similar results were shown for Co and Fe. It was concluded that with the increase of temperature, the activity of citrate ion decreased, resulting in lowering the recoveries [18]. Hence, the experiments are best suited for ambient conditions only. The recovery was found to be 99.0%, 89.2%, 94%, and 99.2% of Cu, Ni, Co, and Fe, respectively, at 308 K (35 °C), using 15% pulp density, 2 N citric acid, and 120 rpm. At 318 K (45 °C), the recovery was found to be 70.9%, 78.3%, 78.9%, and 69.8% of Cu, Ni, Co, and Fe, respectively. The recovery was found to be 48.3%, 59.2%, 64.1%, and 57.5% of Cu, Ni, Co, and Fe, respectively at 328 K (55 °C).
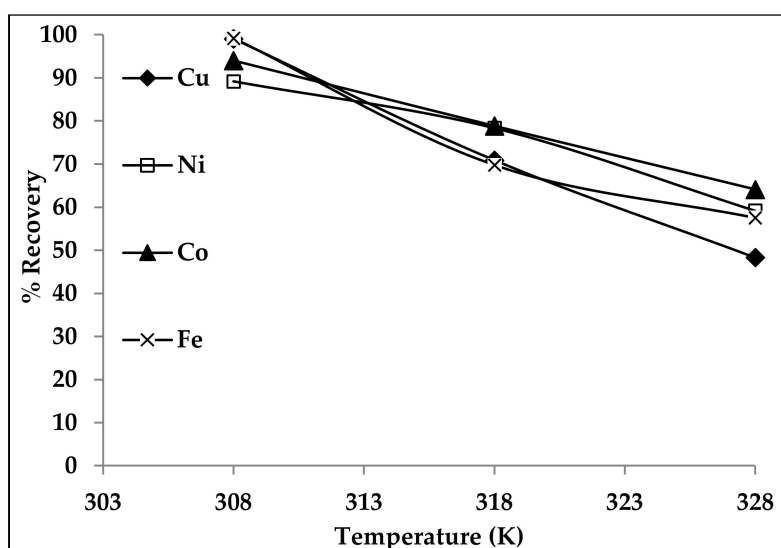

Figure 11. Effect of temperature (308–328 K) on recovery of Cu, Ni, Co, and Fe at 15% pulp density using 2 N citric acid in 15 h.

3.10. Kinetic Models for Leaching of Metals

The rates of metal dissolution were tested against chemical control and diffusion control models. Attempts were made to fit the kinetic data to diffusion control and chemical control models [19]. The kinetic data (Figure 12a–d) appeared to fit well into the chemical-controlled shrinking core model. On the other hand, kinetic data did not show a fit to the diffusion-controlled model for chemical reaction (Figure 13a–d). The high R^2 values (0.98–0.99) at the three temperatures (Figure 11) indicate that dissolution of Cu, Ni, Co, and Fe proceeded by the chemical reaction occurring at the slag surface with citric acid. The rate constant values for the leaching of copper were obtained from Figure 12 as 0.055, 0.039, and 0.033 h^{-1} at 308 K (35 °C), 318 K (45 °C), and 328 K (55 °C), respectively. The rate constant values for the leaching of nickel were obtained from Figure 12 as 0.025, 0.019, and 0.015 h^{-1} at 308 K (35 °C), 318 K (45 °C), and 328 K (55 °C), respectively. The rate constant values for the leaching of cobalt were obtained as 0.035, 0.02 m, and 0.018 h^{-1} at 308 K (35 °C), 318 K (45 °C), and 328 K (55 °C), respectively. Likewise, the rate of constant values for the leaching of iron was obtained as 0.038, 0.028, and 0.025 h^{-1} at 308 K (35 °C), 318 K (45 °C), and 328 K (55 °C), respectively. The recovery of metals was plotted with a diffusion control model too, wherein Figure 13a–d depicts much lower values of correlation coefficient and lower rate constant values of 0.03–0.05 h^{-1} for Cu, 0.01–0.02 h^{-1} for Ni, 0.02–0.03 h^{-1} for Co, and 0.02–0.03 h^{-1} for Fe in the temperature range of 308–328 K (35–55 °C). It depicts the surface-controlled chemical leaching of metals from the iron-silicate matrix, which was further corroborated by SEM and XRD analysis.
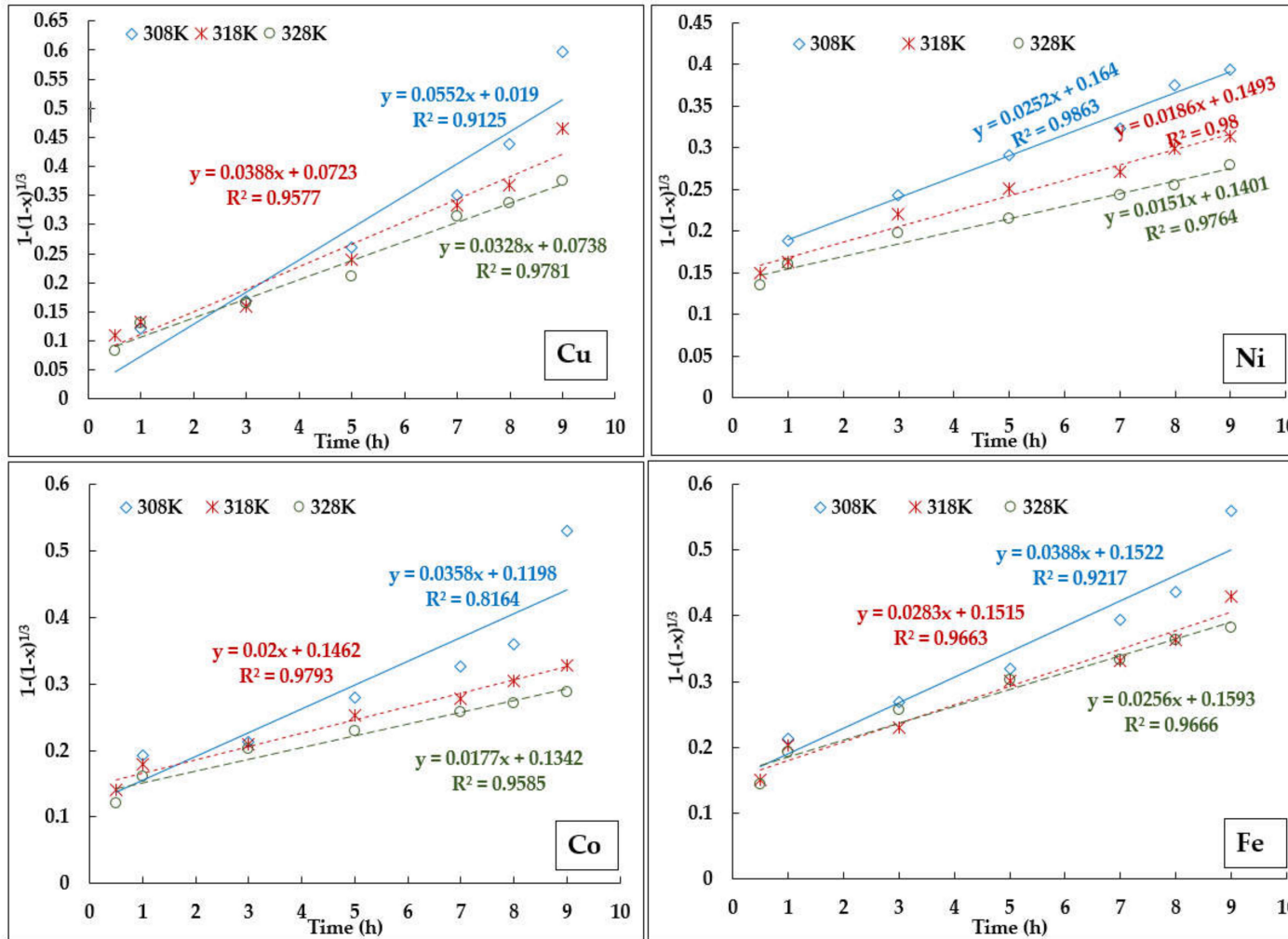
Figure 12. Chemical control model for leaching of Cu, Ni, Co, and Fe from converter slag using 2 N citric acid in temperature range (308–328 K).
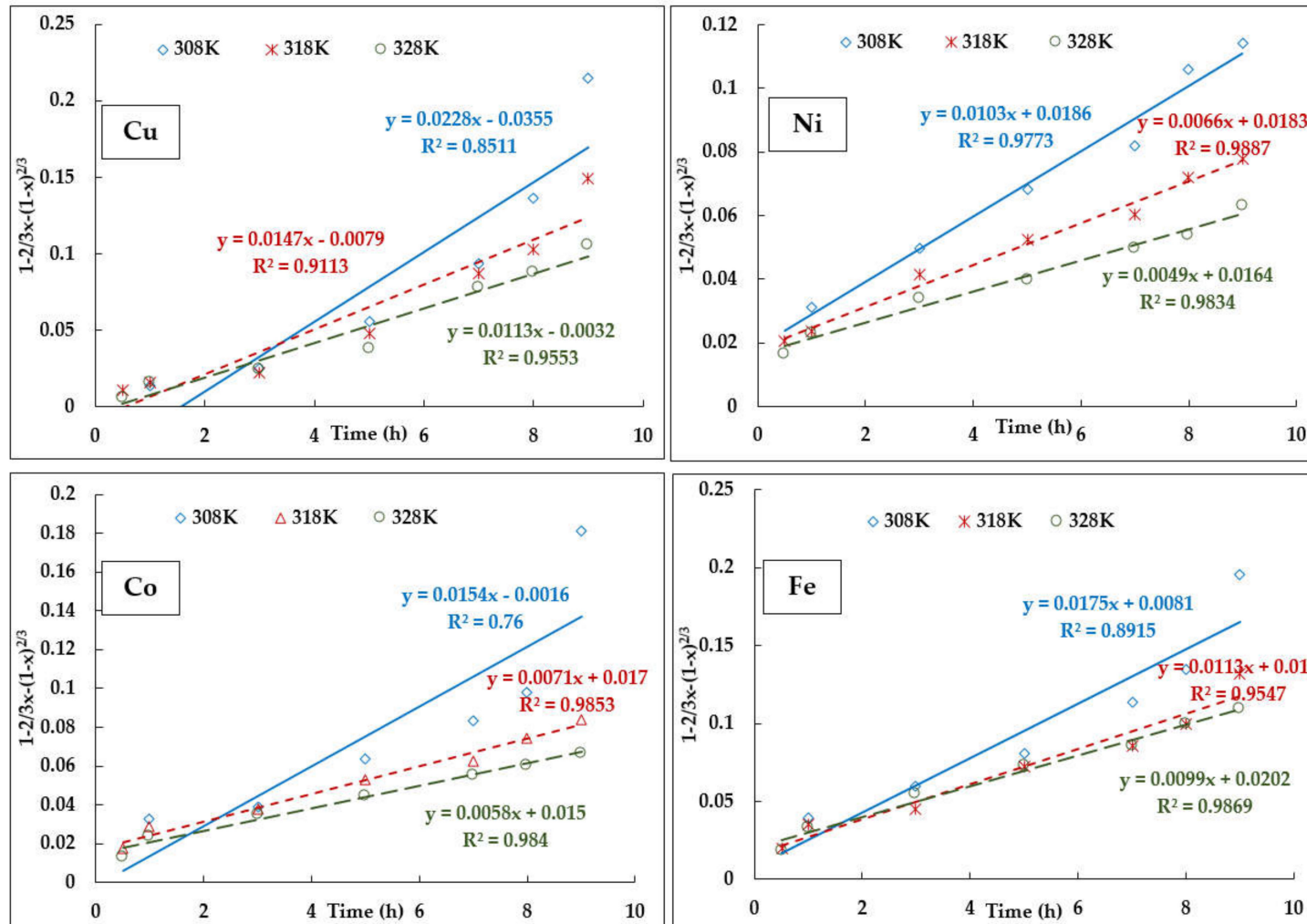
Figure 13. Diffusion control model for leaching of Cu, Ni, Co, and Fe from converter slag using 2 N citric acid in temperature range (308–328 K).

From the Arrhenius plot given in Figure 14, the activation energy values were calculated as 11.3, 13.2, 12.8, and 9.6 kJ/mol, which is well within the range of chemical-controlled reaction for Cu, Ni, Co, and Fe; and is not concurrent within the range of diffusion-controlled reaction (figure not shown). The mechanism of leaching of Cu, Ni, Co, and Fe from slag was further studied by XRD phase identification of the leach residues vis-à-vis the head sample, followed by observing the surface morphology through Scanning Electron Microscopy–X-ray energy dispersive (SEM-EDAX) studies. The leach liquor containing copper, nickel, iron, and cobalt can be subjected to an established process to remove iron by precipitation. This enriches Cu, Ni, and Co, which can be crystallized as citrates and calcined as oxides. These mixed oxides either can be a saleable product or dissolved in very mild sulfuric acid followed by solvent extraction-cum-electrowinning.
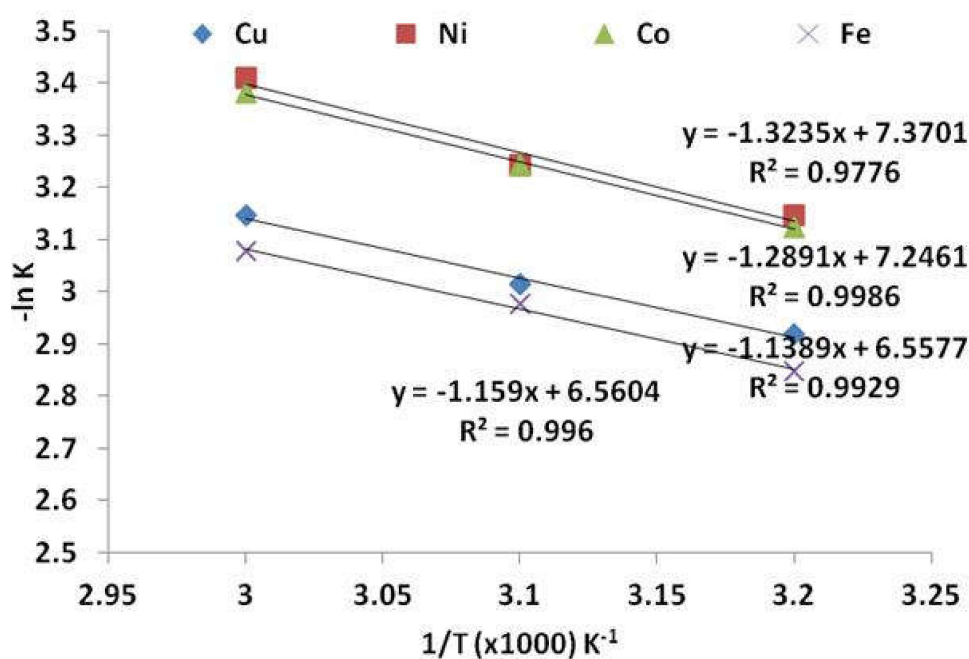

Figure 14. Arrhenius plot for chemical-controlled leaching of Cu, Ni, Co, and Fe from converter slag using 2 N citric acid in temperature range (308–328 K).

4. Discussion

The mechanism of leaching and characterization of the head sample and residue is discussed. The XRD data (Table 5) of the head sample showed fayalite, magnetite, and ferrosilite as major phases and pyrite, bornite, sulfides of copper, nickel, and cobalt as the minor phases. The presence of a silicate phase was found, with the presence of mineral phases of copper, nickel, and cobalt. XRD analysis of leach residue showed the presence of un-reacted predominant iron silicate in the remaining unleached fraction.

Table 5. XRD phase analysis of copper converter slag and residue.

Sample	Major Phases	Minor Phases
Head sample	Fayalite Magnetite Kyanite	Copper silicate Wüstite Oxides of Cu, Ni, Co
Leach residue	Fayalite Pyrite	Fe.O.OH Iron silicate

SEM micrograph (Figure 15) at 308 K (35 °C) shows distinct morphological features with much of the surface exhibiting a high degree of corrosion at 9 h and recording very high (96%) metal recovery.

The chemical reaction on the slag surface with citrate ion is also reflected from the corroded morphology depicting the dissolution of metals from the finely disseminated iron-silicate matrix (cage-like structure). The EDAX analysis shows the higher distribution of silica and iron. The minor base metal in the slag was found non-detrimental to the environment, and the silicate content favors the use of residue as an additive in brick making. The toxicity characteristic leaching procedure (TCLP) tests were carried out as per (United States Environmental Protection Agency (EPA) Standard No. 1311, and after the test the results showed that concentrations of Cu, Ni, and Co in the treated slag were confined below the toxicity limits specified by USEPA and Central Pollution Control Board, India (CPCB) (2018).
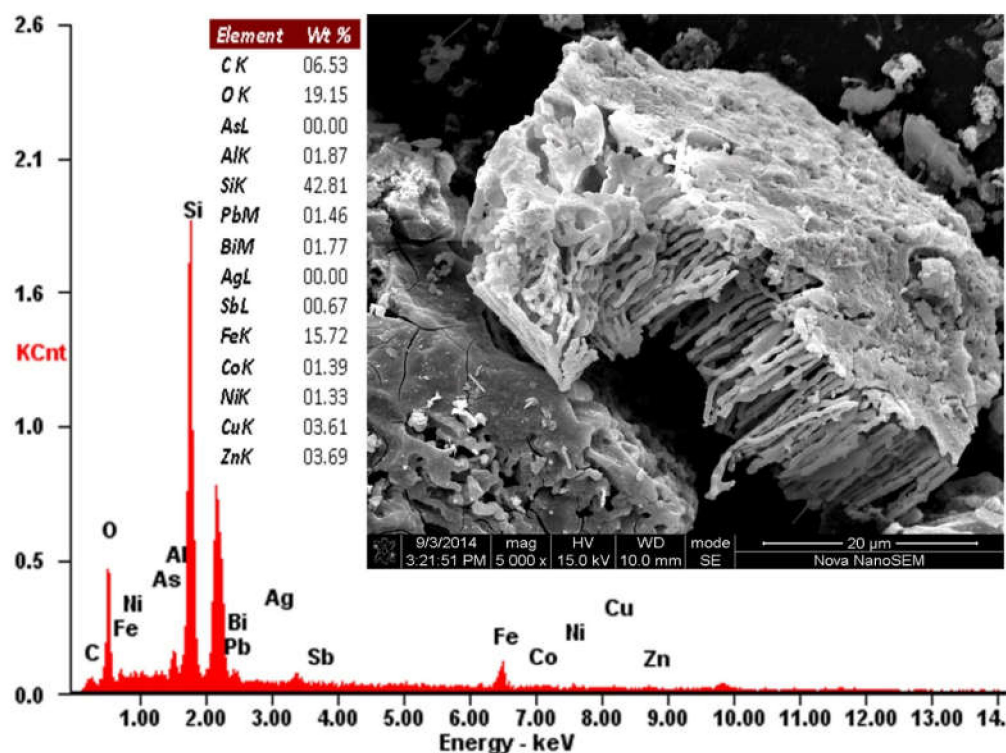

Figure 15. Scanning electron microscope–X-ray energy dispersive (SEM-EDAX) characterization of converter slag after leaching of Cu, Ni, Co, and Fe using 2 N citric acid.

5. Conclusions

This study demonstrates that citric acid leaching at ambient temperature (i.e., 308 K (35 °C)) and normal pressure can effectively be used to extract base metals from copper converter slag. With citric acid, a maximum recovery of 99.0% Cu, 89.2% Ni, 94% Co, and 99.2% Fe is achieved at 15% pulp density in 15 h. Using 2 N oxalic acid recovered only 2.4% Cu, 15.2% Co, and 11.4% Fe, at 5% pulp density, 308 K (35 °C) temperature in 15 h. The Eh-pH values after leaching justify the stability of metal-citrate complex after conversion of copper metal as shown by the Pourbaix diagram of Cu-water-citrate system. The conversion of metals increases as the pulp density increases. The recovery of Cu, Ni, Co, and Fe was almost marginally changed after 9 h after which a steady-state was achieved with 97.5%, 86.7%, 91.6%, and 97.6%, respectively, for Cu, Ni, Co, and Fe. The rate and efficiency of metal recovery decreased with an increase in temperature. The rise in temperature from 308 K (35 °C) to 328 K (55 °C) resulted in a decrease in the conversion of more than 0.5-fold Cu and 0.35-fold Ni, and similar results were shown for Co and Fe. This can be attributed to the lowering of the activity of citrate ions with the increase of temperature. The high values of the correlation coefficient at the three temperatures indicate the dissolution of Cu, Ni, Co, and Fe proceeded by the chemical reaction occurring at the slag surface with citric acid, which was further corroborated with lower values of activation energies, which is well within the range of chemical-controlled reaction. The comparison of

XRD of the leach residues vis-à-vis the head sample showed predominantly un-reacted iron silicate in the residue. FESEM analysis of residue shows distinct morphological features with much of the surface exhibiting a high degree of corrosion by the dissolution of metals from the finely disseminated iron-silicate matrix (cage-like structure).

References

1. Gorai, B.; Jana, R.K.; Premchand. Characteristics and utilisation of copper slag: A review. *Resour. Conserv. Recycl.* **2003**, *39*, 299–313.

2. Agrawal, A.; Sahu, K.K.; Pandey, B.D. Solid waste management in nonferrous industries in India. *Resour. Conserv. Recycl.* **2003**, *42*, 99–120. [CrossRef]

3. Song, S.; Sun, W.; Wang, L.; Liu, R.; Han, H.; Hu, Y.; Yang, Y. Recovery of cobalt and zinc from the leaching solution of zinc smelting slag. *J. Environ. Chem. Eng.* **2019**, *7*, 102777. [CrossRef]

4. Altundogan, H.S.; Boyrazli, M.; Tumen, F. A study on the sulphuric acid leaching of copper converter slag in the presence of dichromate. *Miner. Eng.* **2004**, *17*, 465–467. [CrossRef]

5. Banza, A.N.; Gock, E.; Kongolo, K. Base metals recovery from copper smelter slag by oxidising leaching and solvent extraction. *Hydrometallurgy* **2002**, *67*, 63–69. [CrossRef]

6. Altundogan, H.S.; Tumen, F. Metal recovery from copper converter slag by roasting with ferric sulphate. *Hydrometallurgy* **1997**, *44*, 261–267. [CrossRef]

7. Deng, T.; Ling, Y. Processing of copper converter slag for metal reclamation: Part I: Extraction and recovery of copper and cobalt. *Waste Manag. Res.* **2007**, *25*, 440–448. [CrossRef] [PubMed]

8. Khalid, M.K.; Hamuyuni, J.; Agarwal, V.; Pihlasalo, J.; Haapalainen, M.; Lundström, M. Sulfuric acid leaching for capturing value from copper rich converter slag. *J. Clean. Prod.* **2019**, *215*, 1005–1013. [CrossRef]

9. Mehta, K.D.; Pandey, B.D.; Premchand. Bio-leaching of copper, nickel, and cobalt from copper converter slag by *Thiobacillus ferrooxidans*. *NML Tech. J.* **1997**, *39*, 59–70.

10. Potysz, A.; Kierczak, J. Prospective (bio)leaching of historical copper slags as an alternative to their disposal. *Minerals* **2019**, *9*, 542. [CrossRef]

11. Sukla, L.B.; Kar, R.N.; Panchanadikar, V.V. Bioleaching of copper converter slag using *Aspergillus niger* isolated from lateritic nickel ore. *Int. J. Environ. Stud.* **1995**, *47*, 81–86. [CrossRef]

12. Potysz, A.; Lens, P.N.; van de Vossenberg, J.; Rene, E.R.; Grybos, M.; Guibaud, G.; van Hullebusch, E.D. Comparison of Cu, Zn and Fe bioleaching from Cu-metallurgical slags in the presence of *Pseudomonas fluorescens* and *Acidithiobacillus thiooxidans*. *Appl. Geochem.* **2016**, *68*, 39–52. [CrossRef]

13. Yang, Z.; Rui-lin, M.; Wang-dong, N.; Hui, W. Selective leaching of base metals from copper smelter slag. *Hydrometallurgy* **2010**, *103*, 25–29. [CrossRef]

14. Gargul, K.; Jarosz, P.; Małecki, S. Leaching of Lead and Copper by Citric Acid from Direct-to-Blister Copper Flash Smelting Slag. *Preprints* **2018**, 2018110209. [CrossRef]

15. Meshram, P.; Bhagat, L.; Prakash, U.; Pandey, B.D.; Abhilash. Organic acid leaching of base metals from copper granulated slag and evaluation of mechanism. *Can. Metall. Q.* **2017**, *56*, 168–178. [CrossRef]

16. Lowalekar, V.P. Oxalic Acid-Based Chemical Systems for Electrochemical Mechanical Planarization of Copper. Ph.D. Thesis, University of Arizona, Tucson, AZ, USA, 2006.

17. Adam, F.I.; Bounds, P.L.; Kissner, R.; Koppenol, W.H. Redox properties and activity of iron-citrate complexes: Evidence for redox cycling. *Chem. Res. Toxicol.* **2015**, *28*, 604–614. [CrossRef] [PubMed]

18. Saidan, M.; Linkson, P.; Valix, M. Secondary reaction in the e-waste bioleaching. In Proceedings of the Chemeca 2011, Sydney, Australia, 18–21 September 2011; pp. 575–586.
19. Abhilash; Mehta, K.D.; Pandey, B.D. Bacterial leaching kinetics for copper dissolution from a low-grade Indian chalcopyrite ore. *Rev. Esc. Minas* **2013**, *66*, 245–250. [CrossRef]